This article has been accepted for publication in a future issue of this journal, but has not been fully edited. Content may change prior to final publication. Citation information: DOI 10.1109/ACCESS.2018.2889877, IEEE Access

IEEE Access
Multidisciplinary | Rapid Review | Open Access Journal

Digital Object Identifier

Controllable Sparse Antenna Array for Adaptive Beamforming

WANLU SHI[1], YINGSONG LI[1,2],(Member, IEEE), LUYU ZHAO[3],(Member, IEEE) XIAOGUANG LIU[4],(Senior Member, IEEE)

[1]College of Information and Communication Engineering, Harbin Engineering University, Harbin 150001, China (e-mail: shiwanlu@hrbeu.edu.cn)
[2]Key Laboratory of Microwave Remote Sensing, National Space Science Center, Chinese Academy of Sciences, Beijing 100190, China (e-mail: liyingsong@ieee.org)
[3]Key Laboratory of Antennas and Microwave Technologies, Xidian University, Xi'an 710071, China
[4]Electrical and Computer Engineering, University of California, Davis (email: lxgliu@ucdavis.edu)

Corresponding author: Yingsong Li (e-mail: liyingsong@ieee.org).

This paper is supported by the National Key Research and Development Program of China (2016YFE0111100), Key Research and Development Program of Heilongjiang (GX17A016), the Science and Technology innovative Talents Foundation of Harbin (2016RAXXJ044), the Natural Science Foundation of Beijing (4182077), China Postdoctoral Science Foundation (2017M620918), the Natural Science Foundation of China (61701366) and the Fundamental Research Funds for the Central Universities (HEUCFM180806).

ABSTRACT We propose an l_0-norm constrained normalized least-mean-square (L_0-CNLMS) adaptive beamforming algorithm for controllable sparse antenna arrays. To control the sparsity of the antenna array, an l_0-norm penalty is used as a constraint in the CNLMS algorithm. The proposed algorithm inherits the advantages of CNLMS algorithm in beamforming. The l_0-norm constraint (NC) (l_0-NC) can force the quantities of antennas to a certain number to control the sparsity by selecting a suitable parameter. In addition, the proposed algorithm accelerates the convergence process compared with the existing algorithms in sparse array beamforming and its convergence is presented in this paper. To reduce the computation burden, an approximating l_0-norm method is employed. The performance of the proposed algorithm is analyzed through simulations for various array configurations.

INDEX TERMS l_0-norm; sparse controllable array; NLMS algorithm; constrained adaptive beamforming

I. INTRODUCTION

BEAMFORMING is an important application of array processing and is widely used in radar, sonar, mobile communications, seismic sensing, biomedical engineering and other fields. The formed beam realizes high gain in the desired direction and suppresses interferences in other directions so as to enhance signal-to-interference-plus-noise ratio (SINR). The linearly constrained minimum variance (LCMV) algorithm introduced by Frost [1] is a famous beamforming method for creating a beam in the desired direction and forming a null in the direction of the interfering signal. The LCMV algorithm minimizes the output power with the objective of minimizing the contribution of undesired interference and maintains a constant gain in the direction of observation. Adaptive beamforming algorithms adjust the weighted vectors of the antenna array to match the time-varying signals and interferences. The classic beamforming algorithm CNLMS is a normalized adaptive version of L-CMV, which was derived with the assumption that array elements can be adjusted in real-time [2].

In some applications, e.g. radar, large arrays are essential for achieving the desired performance. However, large antenna arrays require intensive computation, complex transceiver architectures and consume a significant amount of power. As a result, existing beamforming algorithms may be limited by the power consumption, cooling requirement, computation resources, and cost, for large arrays. With the recent development in sparse signal processing [3]–[13], a promising approach for solving the problems mentioned above is to force the filter coefficients toward sparsity which in beamforming applications is defined as the proportion of active antenna elements.

Making use of the sparse characteristics which exist in many applications, e.g. wireless communications, speech signal processing, and remote sensing, sparse signal processing shows particular advantage and have drawn remarkable attention in recent years. Motivated by the Least Absolutely Shrinkage and Selection Operator (LASSO) [14] and Compressive Sensing (CS) [15], LMS based algorithms have been introduced for sparse system identification [3]–[5], [16]–[18]. Among these algorithms, the zero-attracting LMS (ZA-LMS) and the reweighted zero-attracting LMS (RZA-LMS) proposed in [3] are representative. In ZA-LMS , an l_1-norm penalty on the filter coefficients is applied to the quadratic cost function of the standard LMS algorithm and results in an modified LMS updating with a zero attractor for all the filter taps. RZA-LMS further improved the filtering performance by considering reweighted step sizes of the zero attractor for different taps. The zero-attracting technique has been also expanded to many other algorithms [19]–[24]. In addition, another type of algorithms for sparse system identification is Proportionate Normalized LMS (PNLMS) and its variations [16]–[18], [25]–[33]. Motivated by CNLMS and the methods of sparse system identification, the l_1-norm linearly constrained normalized LMS (L_1-CNLMS) algorithm and its weighted version (L_1-WCNLMS) are proposed in [34]. L_1-WCNLMS employs an l_1-NC on the filter coefficients to force the weighting vector towards sparsity and is able to form the desired beam using fewer antennas. However, it is not easy to control the sparsity of the array using L_1-WCNLMS algorithm.

Inspired by the L_1-WCNLMS algorithm in [34], we developed an l_0-NC CNLMS (L_0-CNLMS) algorithm with better performance and stability. l_0-NC is a feasible choice because l_0-norm represents the amount of non-zero elements. For example, in CS theory, l_0-norm minimization solution is optimal for sparse signal recovery. In beamforming, the l_0-norm solution has not seen wide-spread use due to its Non-Polynomial (NP) hard problem. Several possible remedies have been proposed [4], [5], [35]–[37]. In [4], an l_0-norm constrained LMS (CLMS) algorithm is proposed for sparse system identification which utilizes an approximative expression of l_0-norm. In [37], different approaches for approximating l_0-norm are introduced to realize sparsity-aware data-selective adaptive filters. In addition, a soft parameter function penalized normalized maximum correntropy criterion (SPF-NMCC) algorithm is proposed for sparse system identification in [5]. In comparison with zero-attracting MCC (ZA-MCC), SPF-NMCC algorithm achieves a better performance which proves that l_0-norm constrained algorithm can speed up the convergence process compared with l_1-norm penalty method [38].

From the above mentioned recent studies, the sparse beamforming can be realized by using norm penalties into the corresponding cost function. In this paper, an approximating l_0-NC is used to develop an L_0-CNLMS algorithm for improving the beamforming performance for controllable sparse antenna arrays. The L_0-CNLMS algorithm can achieve better performance than L_1-WCNLMS algorithm. Similar to the L_1-WCNLMS algorithm, a new convergence factor is developed to dynamically adjust the convergence speed of the algorithm.

The proposed L_0-CNLMS algorithm can reach a large degree of sparsity of down to 20%. The performance of the L_0-CNLMS algorithm is validated by by considering different array shapes and conditions. A comparison between the L_0-CNLMS and the L_1-WCNLMS is provided to demonstrate that the L_0-CNLMS can accelerate the convergence process. The proposed algorithm shows great potential for satellite communication [39], tactical military communication systems [40], and many other applications that use sparse antenna arrays.

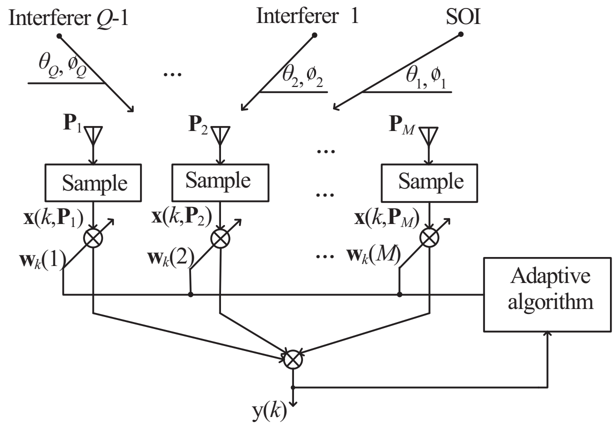

FIGURE 1: Signal processing of planar antenna array.

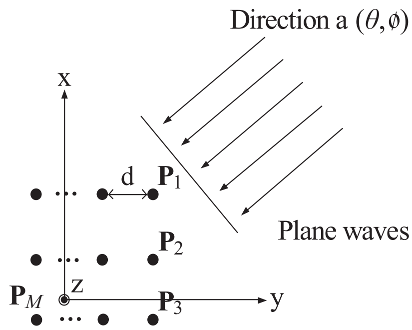

FIGURE 2: Antenna array coordinate graph.

II. MATHEMATICAL MODEL OF ADAPTIVE ARRAY PROCESSING

Figure 1 illustrates a planar antenna array composed of M elements receiving Q far-field signals including interferences and signal of interest (SOI) with wavelength λ and various azimuths (θ_i) and zeniths (ϕ_i) during N snapshots. Since we are interested in only the far field, the signals can be seen as plane waves. Figure 2 shows the arrangement of the planar antenna array.

If we define the data received by the origin of coordinates during the k^{th} snap as $\mathbf{x}(k)$, then the data received by the antennas in other positions $\mathbf{x}(k, \mathbf{P}_m)$ can be obtained through the propagation time-delay τ_m:

$$\begin{cases} \tau_m = \frac{\mathbf{a}_i{}^{\mathrm{T}} \mathbf{p}_m}{c}, \quad m = 1, ..., M, \quad i = 1, \ldots, Q, \\ \mathbf{x}(k, \mathbf{P}_m) = \mathbf{x}(k - \tau_m), \quad k = 1, \ldots, N \\ \mathbf{x}(k) = \sum_{i=1}^{Q} f_i(k) e^{\frac{-j2\pi c}{\lambda} k} + \mathbf{n}(k), \end{cases} \tag{1}$$

where $\mathbf{P}_m$ is the antenna coordinate, c is the propagating speed of signals, $\mathbf{a}_i = [-\sin\theta_i \cos\phi_i, -\sin\theta_i \sin\phi_i]^{\mathrm{T}}$ is

This article has been accepted for publication in a future issue of this journal, but has not been fully edited. Content may change prior to final publication. Citation information: DOI 10.1109/ACCESS.2018.2889877, IEEE Access

a unit vector, θ_i and ϕ_i are the input direction of signals, $f_i(k)$ is the complex envelope of the input signals and $\mathbf{n}(k)$ represents the noise vector. Here, we consider only narrow-band signal whose complex envelope $f_i(k)$ is approximately constant during the time-delay. We can then transform the time-delay information into the variation of phase, i.e., the spatial characteristics of antenna array can be expressed by phase information. As such, the input data during k^{th} snapshot is:

$$\mathbf{x}_k = [\mathbf{x}(k-\tau_1) \quad \mathbf{x}(k-\tau_2) \quad \cdots \quad \mathbf{x}(k-\tau_M)]^{\mathrm{T}}. \quad (2)$$

The output signal y_k during k^{th} snap is:

$$y_k = \mathbf{w}_k^{\mathrm{H}}\mathbf{x}_k, \quad k = 1, \ldots, N, \quad (3)$$

where $\mathbf{w}_k$ is the coefficient vector. So the instantaneous error is $e_k = d_k - y_k$, where d_k represents the desired output signal.

The input signals matrix $\mathbf{X}$ can be defined as:

$$\mathbf{X} = [\ \mathbf{x}_1 \quad \mathbf{x}_2 \quad \cdots \quad \mathbf{x}_N\ ] = \mathbf{AF} + \mathbf{N}, \quad (4)$$

where $\mathbf{A}$ is the $M \times Q$ steering matrix which contains the spatial characteristics information, $\mathbf{F}$ is the $Q \times N$ complex envelope matrix, and $\mathbf{N}$ indicates white noise matrix.

The beam pattern for a direction (θ, ϕ) is:

$$B(\theta,\phi) = \mathbf{w}^{\mathrm{H}} \exp\left\{-j\frac{2\pi\mathbf{a}^{\mathrm{T}}\mathbf{p}_m}{\lambda}\right\}. \quad (5)$$

III. NORM AND SPARSITY

In this paper, an approximate l_0-NC is employed. In CS theory, l_0-norm minimization solution is the optimal solution for sparse signal recovery. However, the l_1-norm, which has the same solution under particular conditions, is popular in many applications because l_0-norm minimization is a NP hard problem. In recent years, many studies on l_0-norm have been proposed [37], [41]. In [37], different approaches for approximating l_0-norm are introduced.

In this paper, l_0-norm is approximated as:

$$||\mathbf{w}(k)||_0 \approx S_\beta(\mathbf{w}(k)) = \sum_{i=0}^{M-1}(1 - e^{-\beta|w_i(k)|}), \quad (6)$$

where parameter β controls the approximation. Figure 3(a) shows the effect of β. As β increases, the curvature of $S_\beta(\mathbf{w}(k))$ becomes sharper. When β is very large, the function is close to l_0-norm.

In order to reduce the computational complexity brought by the exponential function, we use the first order Taylor series expansions of exponential functions [4]:

$$f_\beta(x) = e^{-\beta|x|} = \begin{cases} 1-\beta|x| & \beta|x| \le 1; \\ 0 & \text{elsewhere}, \end{cases} \quad (7)$$

shown in Fig. 3(b), a larger β signifies stronger attraction for small coefficients but less scope width.

One may notice that the sparse adaptive beamforming method proposed in [34] employs an l_1-norm as a constrain to derive the final update formulation. The L_1-WCNLMS is an l_1-norm canonical technique, which is implemented via using the l_1-norm constraint to speed up the convergence procedure.

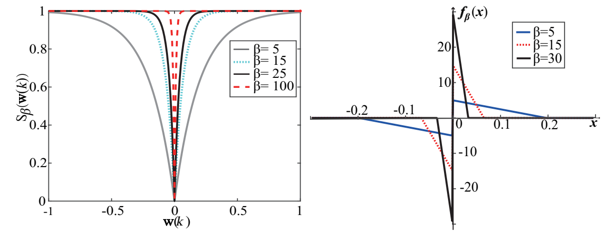

(a) (b)

FIGURE 3: (a) Performance of $S_\beta(\mathbf{w}(k))$ for various parameter β. (b) The curves of function $f_\beta(x)$ with various parameter β.

By applying the approximate expression of the exponential functions, it is obvious that the equation:

$$||\mathbf{w}_k||_0 \approx S_\beta(\mathbf{w}(k)) \approx \mathbf{J}_k^{\mathrm{H}}\mathbf{w}_k, \quad (8)$$

is satisfied in terms of the gradient as $\mathbf{J}_k$, of approximated l_0-norm. Equation (8) is an important condition for the proposed algorithm.

IV. THE CLMS ALGORITHM AND THE CNLMS ALGORITHM

A. THE CLMS ALGORITHM

The solution to the LCMV algorithm introduced in [1], [42] is:

$$\mathbf{w}_{\mathrm{opt}} = \mathbf{R}^{-1}\mathbf{C}(\mathbf{C}^{\mathrm{H}}\mathbf{R}^{-1}\mathbf{C})^{-1}\mathbf{f}, \quad (9)$$

where $\mathbf{R}$, $\mathbf{C}$, $\mathbf{f}$ are the covariance matrix, constrained matrix, constrained vector, respectively. H represents Hermitian operator (conjugate transpose), and the covariance matrix $\mathbf{R}$ is defined as $\mathrm{E}[\mathbf{x}_k\mathbf{x}_k^{\mathrm{H}}]$. It is estimated by the time average.

CLMS algorithm is the adaptive version of LCMV [1], [42]. The target function of CLMS algorithm is:

$$\min_{\mathbf{w}} E\left[|e_k|^2\right] \text{s.t.} \mathbf{C}^{\mathrm{H}}\mathbf{w} = \mathbf{f}. \quad (10)$$

The Lagrange multiplier is used to transform the constrained optimization problem for the solution of unconstrained extreme value problem. The cost function is:

$$L_k^{clms} = E\left[|e_k|^2\right] + \boldsymbol{\gamma}_1^{\mathrm{H}}(\mathbf{C}^{\mathrm{H}}\mathbf{w} - \mathbf{f}). \quad (11)$$

By using the steepest descent method, the coefficient vector updating equation at iteration k can be calculated:

$$\mathbf{w}_{k+1} = \mathbf{w}_k - \frac{\mu}{2}\mathbf{g}_{\mathbf{w}}L_k^{clms}, \quad (12)$$

where $\mathbf{g}_{\mathbf{w}}L_k^{clms}$ is the gradient vector of L_k^{clms} and points to the steepest rise direction of the cost function [34], [42]:

$$\mathbf{g}_{\mathbf{w}}L_k^{clms} = -2E\left[e_k^*\mathbf{x}_k\right] + \mathbf{C}\boldsymbol{\gamma}_1. \quad (13)$$

In the calculation process, the instantaneous estimate of $\mathrm{E}[\mathbf{x}_k^*\mathbf{x}_k^{\mathrm{H}}]$ is employed:

$$\hat{\mathbf{g}}_{\mathbf{w}} L_k^{clms} = -2e_k^*\mathbf{x}_k + \mathbf{C}\boldsymbol{\gamma}_1. \tag{14}$$

Applying the constrain relation $\mathbf{C}^{\mathrm{H}}\mathbf{w}_{k+1} = \mathbf{f}$, $\boldsymbol{\gamma}_1$ can be solved. Finally, the updating equation for CLMS algorithm is:

$$\mathbf{w}_{k+1} = \mathbf{P}\left[\mathbf{w}_k + \mu e_k^*\mathbf{x}_k\right] + \mathbf{f}_c, \tag{15}$$

with:

$$\begin{cases} \mathbf{P} = \mathbf{I}_{M\times M} - \mathbf{C}\left(\mathbf{C}^{\mathrm{H}}\mathbf{C}\right)^{-1}\mathbf{C}^{\mathrm{H}}, \\ \mathbf{f}_c = \mathbf{C}\left(\mathbf{C}^{\mathrm{H}}\mathbf{C}\right)^{-1}\mathbf{f}, \end{cases} \tag{16}$$

where $\mathbf{P}$ is a symmetric projection matrix, $\mathbf{f}_c$ is an $M\times 1$ vector, $\mathbf{I}$ is the unit matrix, and μ is the convergence factor. Because $\mathbf{w}_k$ was forced to satisfy the constraint in (10), it is obvious that the following equation is satisfied [2]:

$$\mathbf{P}\mathbf{w}_k + \mathbf{f}_c = \mathbf{w}_k. \tag{17}$$

B. THE CNLMS ALGORITHM

To accelerate the convergence of CLMS algorithm, the normalized version CNLMS algorithm is proposed [2]. A feasible method is to reduce the instantaneous error $e_{ap}(k) = d_k - \mathbf{x}_k^{\mathrm{H}}\mathbf{w}_{k+1}$ as much as possible during each iteration. As a result, a variable μ_k is used to replace the constant μ [2], [34], [42].

Considering (15) and (17), we obtain:

$$e_{ap}(k) = e_k\left(1 - \mu_k\mathbf{x}_k^{\mathrm{H}}\mathbf{P}\mathbf{x}_k\right). \tag{18}$$

To minimize $e_{ap}(k)$, we use the partial derivative of $e_{ap}^2(k)$ with respect to μ_k:

$$\frac{\partial\left[|e_{ap}(k)|^2\right]}{\partial\mu_k^*} = \frac{\partial\left[e_{ap}(k)e_{ap}^*(k)\right]}{\partial\mu_k^*} = 0. \tag{19}$$

According to [42]:

$$\frac{\partial\left[|e_ap(k)|^2\right]}{\partial\mu_k^*} = \frac{1}{2}\left[\frac{\partial|e_{ap}(k)|^2}{\partial\Re\mu_k} + j\frac{\partial|e_{ap}(k)|^2}{\partial\Im\mu_k}\right], \tag{20}$$

where $\Re\mu_k$ and $\Im\mu_k$ are the real and imaginary parts of μ_k. (19) can then be transformed as:

$$\frac{\partial\left[|e_{ap}(k)|^2\right]}{\partial\mu_k^*} = \frac{e_{ap}(k)}{2}\left[\frac{\partial e_{ap}^*(k)}{\partial\Re\mu_k} + j\frac{\partial e_{ap}^*(k)}{\partial\Im\mu_k}\right]. \tag{21}$$

Then, we can obtain

$$\mu_k = \frac{\mu_0}{\mathbf{x}_k^{\mathrm{H}}\mathbf{P}\mathbf{x}_k + \epsilon}, \tag{22}$$

where the parameter ϵ is positive to avoid excessive step size when $\mathbf{x}_k^{\mathrm{H}}\mathbf{P}\mathbf{x}_k$ is too small. Finally, the CNLMS algorithm coefficients updating function is:

$$\mathbf{w}_{k+1} = \mathbf{P}\left[\mathbf{w}_k + \mu_0\frac{e_k\mathbf{x}_k}{\mathbf{x}_k^{\mathrm{H}}\mathbf{P}\mathbf{x}_k + \epsilon}\right] + \mathbf{f}. \tag{23}$$

V. THE PROPOSED L_0-CNLMS ALGORITHM

A. ALGORITHM DERIVATIVE PROCESS

In [4], an l_0-norm penalty on the filter coefficients is incorporated to the cost function of LMS algorithm to speed up coefficient shrinkage. In [43], an l_1-norm penalty is added to the constrain list of CLMS algorithm to enhance sparsity.

In this paper, an l_0-norm is utilized. The objective function is:

$$\min_{\mathbf{w}} E\left[|e_k|^2\right] \quad \text{s.t.} \begin{cases} \mathbf{C}^{\mathrm{H}}\mathbf{w} = \mathbf{f}; \\ ||\mathbf{w}||_0 = t, \end{cases} \tag{24}$$

where $||\cdot||_0$ denotes l_0-norm that counts the number of non-zero entries in $\mathbf{w}$, and t is the constrain of $||\mathbf{w}||_0$.

The cost function is:

$$L_k^{l_0} = E\left[|e_k|^2\right] + \boldsymbol{\gamma}_1^{\mathrm{H}}\left(\mathbf{C}^{\mathrm{H}}\mathbf{w} - \mathbf{f}\right) + \gamma_{l_0}\left[||\mathbf{w}||_0 - t\right]. \tag{25}$$

According to (6), the proposed cost function can be written as:

$$\begin{aligned} L_k^{l_0} =& E\left[|e_k|^2\right] + \boldsymbol{\gamma}_1^{\mathrm{H}}\left(\mathbf{C}^{\mathrm{H}}\mathbf{w} - \mathbf{f}\right) \\ &+ \gamma_{l_0}\left[\sum_{i=0}^{M-1}\left(1 - e^{-\beta|w_i(k)|}\right) - t\right]. \end{aligned} \tag{26}$$

The instantaneous estimate of the gradient $L_k^{l_0}$ in (26) is expressed as:

$$\begin{cases} \mathbf{g}_{\mathbf{w}}\varepsilon(\mathbf{w}) = -2e_k^*\mathbf{x}_k + \mathbf{C}\boldsymbol{\gamma}_1 + \gamma_{l_0}\mathbf{J}_k, \\ \mathbf{J}_k = \beta\left[\mathrm{sgn}(w_1)(1-\beta|w_1|), \cdots, \mathrm{sgn}(w_M)(1-\beta|w_M|)\right]^{\mathrm{T}}. \end{cases} \tag{27}$$

where $\mathrm{sgn}(\cdot)$ is an element-wise sign operator, which is defined as:

$$\mathrm{sgn}(x) = \begin{cases} \frac{x}{|x|} & x \neq 0; \\ 0 & \text{elsewhere}. \end{cases} \tag{28}$$

According to the steepest descent method, the coefficients updating equation can be written as:

$$\mathbf{w}_{k+1} = \mathbf{w}_k - \frac{\mu}{2}\left\{-2e_k^*\mathbf{x}_k + \mathbf{C}\boldsymbol{\gamma}_1 + \gamma_{l_0}\mathbf{J}_k\right\}. \tag{29}$$

Next, we use constraints in (24) to eliminate $\boldsymbol{\gamma}_1$ and γ_{l_0}. Here, we assume that the algorithm has converged, i.e. $\mathbf{w}_{k+1} = \mathbf{w}_k$. The approximation $\mathbf{J}_k^{\mathrm{H}}\mathbf{w}_{k+1} = t$ is proposed in [34], as $\mathbf{w}_k$ and $\mathbf{w}_{k+1}$ are expected to be in the same hyper-quadrant. Then the constraints can be written as:

$$\begin{cases} \mathbf{C}^{\mathrm{H}}\mathbf{w}_{k+1} = \mathbf{C}^{\mathrm{H}}\mathbf{w}_k = \mathbf{f} & \text{(30a)} \\ \mathbf{J}_k^{\mathrm{H}}\mathbf{w}_{k+1} = t. & \text{(30b)} \end{cases}$$

Using (30a), $\boldsymbol{\gamma}_1$ can be solved premultiplying (29) by $\mathbf{C}^{\mathrm{H}}$:

$$\boldsymbol{\gamma}_1 = \mathbf{G}\left(2e_k^*\mathbf{x}_k - \gamma_{l_0}\mathbf{J}_k\right), \tag{31}$$

where $\mathbf{G} = (\mathbf{C}^{\mathrm{H}}\mathbf{C})^{-1}\mathbf{C}^{\mathrm{H}}$.

Using (30b) and applying (8), l_0-norm is denoted as $t_k = \mathbf{J}_k^{\mathrm{H}}\mathbf{w}_k$. Multiplying (29) by $\mathbf{J}_k^{\mathrm{H}}$:

$$t = t_k - \frac{\mu}{2}\left\{-2e_k^*\mathbf{J}_k^{\mathrm{H}}\mathbf{x}_k + \mathbf{J}_k^{\mathrm{H}}\mathbf{C}\boldsymbol{\gamma}_1 + \gamma_2 n\right\}, \tag{32}$$

where n=$\mathbf{J}_k^{\mathrm{H}}\mathbf{J}_k$ is a scalar.

This article has been accepted for publication in a future issue of this journal, but has not been fully edited. Content may change prior to final publication. Citation information: DOI 10.1109/ACCESS.2018.2889877, IEEE Access

Defining l_0-norm error as $e_{L_0}(k) = t - t_k$, and substituting (31) to (32), γ_{l_0} can be solved:

$$\gamma_{l_0} = -\frac{2}{m\mu} e_{L_0}(k) + \frac{2e_k^* \mathbf{J}_k^{\mathrm{H}} \mathbf{P} \mathbf{x}_k}{m}, \tag{33}$$

where $m = \mathbf{J}_k^{\mathrm{H}} \mathbf{P} \mathbf{J}_k$ is a scalar.

Taking $\boldsymbol{\gamma}_1$ and γ_{l_0} into (29) and making use of (17), we can obtain the update equation for L_0-CLMS:

$$\mathbf{w}_{k+1} = \mathbf{w}_k + \mu_0 e_k^* \mathbf{Q} + \mathbf{f}_{L_0}(k), \tag{34}$$

where:

$$\begin{cases} \mathbf{P} = \mathbf{I}_{M\times M} - \mathbf{C}(\mathbf{C}^{\mathrm{H}}\mathbf{C})^{-1}\mathbf{C}^{\mathrm{H}}, \\ q = \mathbf{J}_k^{\mathrm{H}} \mathbf{P} \mathbf{x}_k, \\ m = \mathbf{J}_k^{\mathrm{H}} \mathbf{P} \mathbf{J}_k, \\ \mathbf{Q} = \mathbf{P}(\mathbf{x}_k - \frac{q\mathbf{J}_k}{m}), \\ e_k = -\mathbf{w}_k^{\mathrm{H}} \mathbf{x}_k, \\ \mathbf{f}_{L_0}(k) = (t - \mathbf{J}_k^{\mathrm{H}} \mathbf{w}_k)(\frac{\mathbf{P}\mathbf{J}_k}{m}). \end{cases} \tag{35}$$

The same approach of CNLMS algorithm can be applied to the L_0-CNLMS algorithm.

According to the update equation of L_0-CLMS algorithm list on (34), we can obtain:

$$e_{ap}(k) = e_k (1 - \mu_k \mathbf{Q} \mathbf{x}_k). \tag{36}$$

Applying (19), (20) and (21), we can get μ_k for the L_0-CNLMS algorithm:

$$\mu_k = \frac{\mu_0 [e_k - \mathbf{f}_{L_0}^{\mathrm{H}}(k) \mathbf{x}_k]}{e_k \mathbf{Q}^{\mathrm{H}} \mathbf{x}_k + \epsilon}. \tag{37}$$

The final updating function of L_0-CNLMS algorithm is:

$$\mathbf{w}_{k+1} = \mathbf{w}_k + \mu_k e_k^* \mathbf{Q} + \mathbf{f}_{L_0}(k), \tag{38}$$

where:

$$\begin{cases} \mathbf{P} = \mathbf{I}_{M\times M} - \mathbf{C}(\mathbf{C}^{\mathrm{H}}\mathbf{C})^{-1}\mathbf{C}^{\mathrm{H}}, \\ q = \mathbf{J}_k^{\mathrm{H}} \mathbf{P} \mathbf{x}_k, \\ m = \mathbf{J}_k^{\mathrm{H}} \mathbf{P} \mathbf{J}_k, \\ \mathbf{Q} = \mathbf{P}(\mathbf{x}_k - \frac{q\mathbf{J}_k}{m}), \\ e_k = -\mathbf{w}_k^{\mathrm{H}} \mathbf{x}_k, \\ \mathbf{f}_{L_0}(k) = (t - \mathbf{J}_k^{\mathrm{H}} \mathbf{w}_k)(\frac{\mathbf{P}\mathbf{J}_k}{m}), \\ \mu_k = \frac{\mu_0 [e_k - \mathbf{f}_{L_0}^{\mathrm{H}}(k) \mathbf{x}_k]}{e_k \mathbf{Q}^{\mathrm{H}} \mathbf{x}_k + \epsilon}. \end{cases} \tag{39}$$

The final algorithm is expressed via pseudo-codes in Algorithm 1.

The computational complexity of the proposed L_0-CNLMS in each iteration is given in Table 1 under the assumption that $Q = 1$. It can be seen that the complexity of the proposed L_0-CNLMS is O(M) which is similar to that of CNLMS. However, the proposed L_0-CNLMS is superior to the CNLMS and the L_1-WCNLMS with respect to the convergence and the performance for sparse array beamforming, which will be verified in next section.

In our proposed L_0-CNLMS algorithm, we aim to develop an l_0-norm based sparse adaptive beamforming method, which exploits the sparse characteristic of the array while keeping the same beam patterns with previous adaptive beamforming algorithms. We use the l_0-norm constraint in the new cost function to get the derivation of the proposed L_0-CNLMS algorithm in detail. Since the l_0-norm is an approximation for getting a close solution of l_0-norm constraint due to the NP-hard problem, other l_0-norm approximation can be used for smoothing the l_0-norm, such as smooth l_0-norm in compressed sensing [15], [36], l_0-norm in adaptive filters [4]. In the L_0-CNLMS algorithm, we introduce the l_0-norm to create a new cost function since the l_0-norm constraint can directly get the active array elements to accelerate the convergence and achieve a better sparse beamforming. The derivation of the proposed algorithm is based on the gradient descent method which has been found in the adaptive filter and adaptive beamforming algorithms [9]–[11], [34], [43]. In addition, our proposed L_0-CNLMS utilizes two different constraints to obtain the high gain and sparsity of the array. Thus, the active antenna array elements can be controlled to realize sparse array with reliable and controllable beam patterns.

Algorithm 1 Algorithm for L_0-CNLMS

Input: t, μ_0, k, β, in
Output: $\mathbf{w}$ out
Initialisation :
$\mathbf{P} = \mathbf{I}_{M\times M} - \mathbf{C}(\mathbf{C}^{\mathrm{H}}\mathbf{C})^{-1}\mathbf{C}^{\mathrm{H}}$;
$\mathbf{f}_c = \mathbf{C}(\mathbf{C}^{\mathrm{H}}\mathbf{C})^{-1}\mathbf{f}$;
$\mathbf{w}(1) = \mathbf{f}_c$;
LOOP Process
while $(k<k_{\max})$ **do**
$e_k = d_k - \mathbf{w}_k^{\mathrm{H}} \mathbf{x}_k$;
$e_{L_0}(k) = t - t_k$;
$\mathrm{J}_k = \beta[\mathrm{sgn}[w_1](1-\beta|w_1|), \cdots, \mathrm{sgn}[w_M](1-\beta|w_M|)]^{\mathrm{T}}$;
$q = \mathbf{J}_k^{\mathrm{H}} \mathbf{P} \mathbf{x}_k$;
$m = \mathbf{J}_k^{\mathrm{H}} \mathbf{P} \mathbf{J}_k$;
$\mathbf{Q} = \mathbf{P}(\mathbf{x}_k - \frac{q\mathbf{J}_k}{m})$;
$\mathbf{f}_{L_0}(k) = (t - \mathbf{J}_k^{\mathrm{H}} \mathbf{w}_k)(\frac{\mathbf{P}\mathbf{J}_k}{m})$;
$\mu_k = \frac{\mu_0 [e_k - \mathbf{f}_{L_0}^{\mathrm{H}}(k) \mathbf{x}_k]}{e_k \mathbf{Q}^{\mathrm{H}} \mathbf{x}_k + \epsilon}$;
$\mathbf{w}_{k+1} = \mathbf{w}_k + \mu_k e_k^* \mathbf{Q} + \mathbf{f}_{L_0}(k)$;
end while
return $\mathbf{w}$

TABLE 1: Complex Operations in Each Iterations

Algorithm	Additions	Divisions	Multiplications
CNLMS	$3M-3$	1	$3M+1$
L_1-WCNLMS	$16M+5$	$M+3$	$13M+6$
L_0-CNLMS	$15M+5$	$M+2$	$12M+5$

B. ALGORITHM WORKING PROCESS

From equation (24), we can see that the proposed L_0-CNLMS algorithm has two constraints, where one is used for obtaining high gain and suppressing the interferences while the other one is to exploit the sparsity. In our proposed algorithm, we aim to propose sparse controllable beamforming algorithm to use less active array elements and to achieve

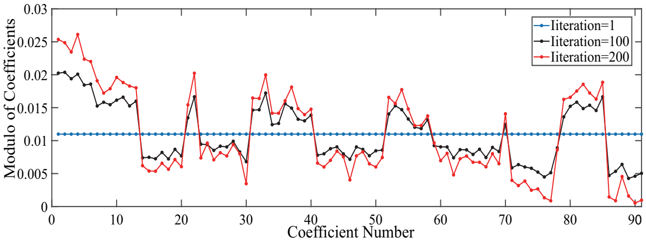

FIGURE 4: Algorithm working process.

TABLE 2: Parameter values for SHA simulations

Parameter	I	II	III
L_0-CNLMS step-size (μ_0)	1.8×10^{-4}	1.8×10^{-4}	3×10^{-4}
β	18	20	25
Elements' interval	$\lambda/2$	$\lambda/2$	$\lambda/2$
l_0-NC	0.2	0.5	0.2
Signals' frequencies	8 GHz	8 GHz	8 GHz
SOI SNR (dB)	20	20	20
Interferer SNR (dB)	40	40	40
SOI direction (θ,ϕ)	90°, 45°	90°, 60°	90°, 75°
Interference 1 (θ,ϕ)	36°, 45°	25°, 60°	40°, 75°
Interference 2 (θ,ϕ)	65°, 45°	55°, 60°	130°, 75°
Interference 3 (θ,ϕ)	120°, 45°	130°, 60°	-
Interference 4 (θ,ϕ)	159°, 45°	169°, 60°	-

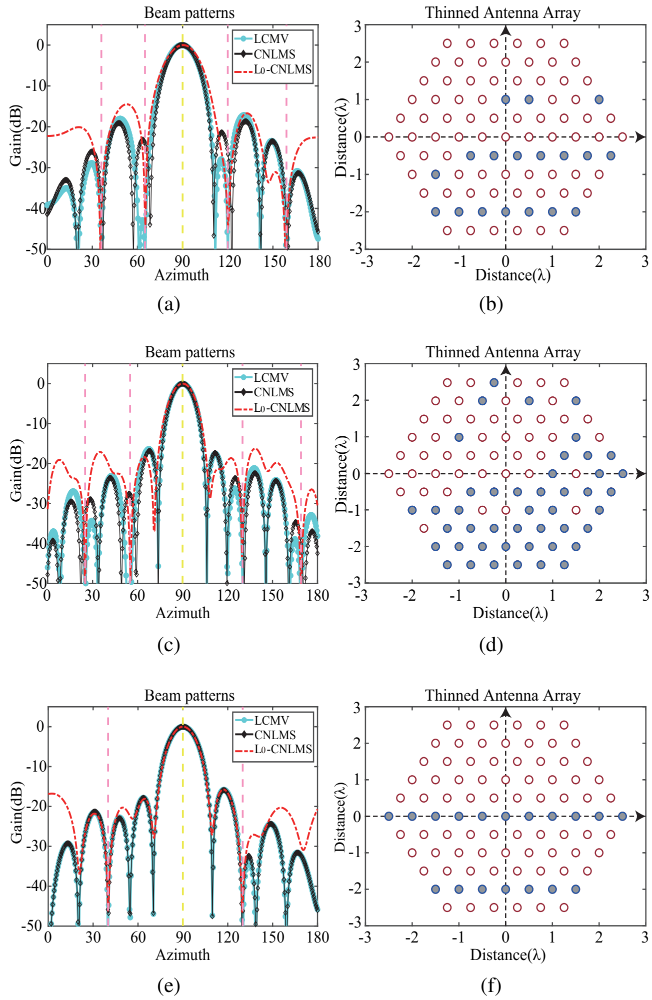

FIGURE 5: SHA simulations: The beam patterns for the L_0-CNLMS compared with CNLMS and LCMV algorithms, pink lines show the directions of interferences, the yellow line is on behalf of the SOI. The thinned array at iteration $k = 6 \times 10^3$, white circles represent the elements turned off by L_0-CNLMS. (a)Simulation I: Beam patterns, (b) Simulation I: Array sparsity = 19.8%, (c)Simulation II: Beam patterns, (d) Simulation II: Array sparsity = 49.5%, (e)Simulation III: Beam patterns, (f) Simulation III: Array sparsity = 19.8%.

acceptable beam pattern performance in comparison with other algorithms. The operating principle of our proposed L_0-CNLMS algorithm is presented in Fig. 4. Since we use the l_0-NC to exploit the sparsity property of the arrays to reduce the active elements and to reduce the computational burden, the small coefficients are attracted to zero without sacrificing the gain of the main lobe. Thus, the active coefficients in the array become larger, which will deteriorate the side lobe level (SLL) and the first null beam width (FNBW).

VI. SIMULATION RESULTS

Simulations are carried out on various array configurations to evaluate the effectiveness of the L_0-CNLMS algorithm for adaptive array beamforming. Then, investigations and comparisons of L_0-CNLMS and L_1-WCNLMS are illustrated to demonstrate the improvement of the proposed algorithm. Interferers and SOI in the experiments are narrowband QP-SK signals. Parameters of the simulations are listed in the following tables.

A. STANDARD HEXAGONAL ARRAY (SHA)

In the first simulation, we consider a SHA receiving signals for satellite communication. Each edge of SHA employs 6 antennas, leading to a total of 91 antennas. The major parameters of the simulation are listed in Table 2. We vary the direction of the signals, the number of the signals, and the sparsity of the antenna array.

Results are shown in Fig. 5 and Fig. 6. The L_0-CNLMS, LCMV and CNLMS algorithms form beams with nearly identical shape in the main lobe and nulls. From the mean-square-error (MSE) and the l_0-norm shown in Figure 6, the MSE performance of the L_0-CNLMS algorithm is better than that of CNLMS. The L_0-CNLMS algorithm converges after 3,000 iterations and achieves similar performance with various signals' zeniths, quantity and directions. The L_0-CNLMS algorithm achieves a sparsity of 19.8%, 49.5%, and 19.8% which equal to the prescribed parameter t of 0.2, 0.5, 0.2.

B. RECTANGULAR ARRAY (RA)

In the second simulation, we consider a 100-element RA receiving C-band signals commonly found in radar systems. The parameters of the simulations are listed in Table 3.

Figure 7 is the result of RA simulation. Detail performances of MSE and l_0-norm are omitted for brevity. We

This article has been accepted for publication in a future issue of this journal, but has not been fully edited. Content may change prior to final publication. Citation information: DOI 10.1109/ACCESS.2018.2889877, IEEE Access

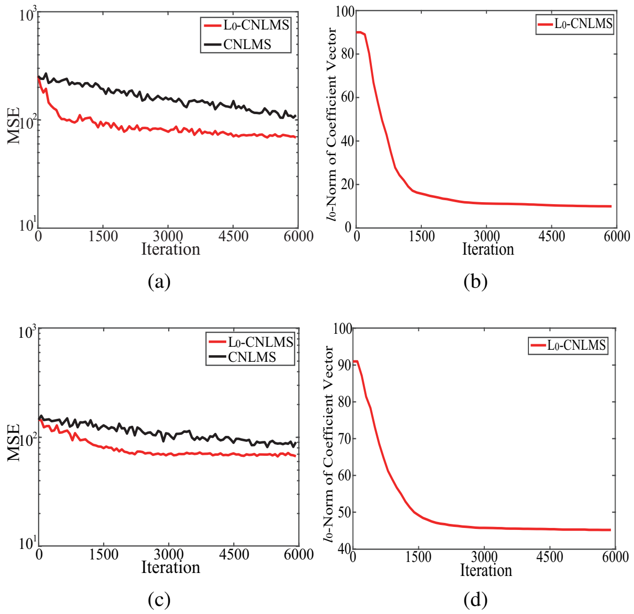

FIGURE 6: SHA simulations: The MSE performance for L_0-CNLMS and CNLMS algorithms and l_0-norm of the coefficient vector at iteration $k = 6 \times 10^3$. (a) Simulation I: MSE, (b)Simulation I: l_0-norm, (c)Simulation II: MSE, (d)Simulation II: l_0-norm.

TABLE 3: Parameter values for RA simulations

Parameter	I	II	III
L_0-CNLMS step-size (μ_0)	8.5×10^{-4}	8×10^{-4}	8×10^{-4}
β	20	20	25
Elements' interval	$\lambda/2$	$\lambda/2$	$\lambda/2$
l_0-NC	0.2	0.4	0.7
Signal frequencies	5 GHz	6 GHz	7 GHz
SOI SNR (dB)	20	20	20
Interferer SNR (dB)	40	40	40
SOI direction (θ,ϕ)	90°, 45°	90°, 75°	90°, 30°
Interference 1 (θ,ϕ)	25°, 45°	13°, 75°	33°, 30°
Interference 2 (θ,ϕ)	50°, 45°	70°, 75°	75°, 30°
Interference 3 (θ,ϕ)	125°, 45°	110°, 75°	150°, 30°
Interference 4 (θ,ϕ)	158°, 45°	174°, 75°	174°, 30°

can conclude from the results that the proposed algorithm can be used in RA properly. Same as SHA, the L_0-CNLMS can deal with the varying conditions successfully and form the ideal beam. Similarly, the sparsity of the antenna arrays are controlled exactly and equal to the parameter t. In this way, we can change the performance of the formed beam through regulating the sparsity of the antenna array which is significant in sparse array beamforming.

C. TRIANGULAR ARRAY (TA)

In this simulation, TA is considered as the senor for P-band signals which has particularly advantage in stealth aircraft and satellite detection. TA in this simulation contains 9 rows where each row consists of 13 elements. The parameters of the simulations are given in Table 4.

As Fig. 8 indicates, the beams are formed successfully against the SOI and interferences, and the sparsity of arrays match the parameter t well.

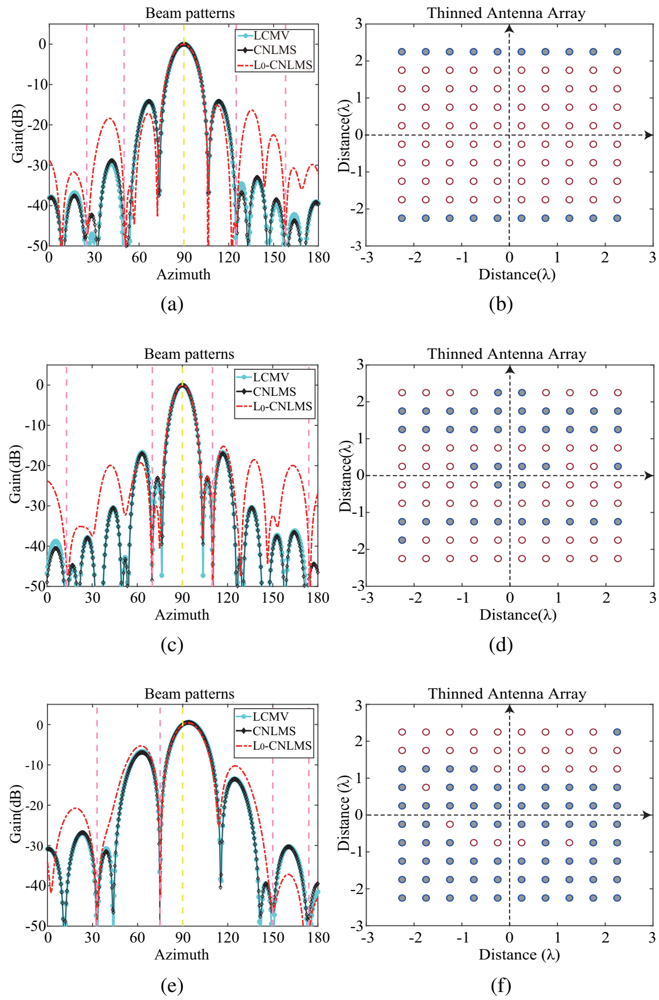

FIGURE 7: RA simulations: The beam patterns for the L_0-CNLMS compared with CNLMS and LCMV algorithms. The thinned array at iteration $k = 3 \times 10^3$. (a) Simulation I: Beam patterns, (b) Simulation I: Array sparsity = 20%. (c) Simulation II: Beam patterns, (d) Simulation II: Array sparsity = 40%, (e) Simulation III: Beam patterns, (f) Simulation III: Array sparsity = 69%.

TABLE 4: Parameter values for TA simulations

Parameter	I	II
L_0-CNLMS step-size (μ_0)	6×10^{-4}	6×10^{-4}
β	18	18
Elements' interval	$\lambda/2$	$\lambda/2$
l_0-NC	0.35	0.55
Signals' frequencies	500 MHz	500 MHz
SOI SNR (dB)	20	20
Interferer SNR (dB)	40	40
SOI direction (θ,ϕ)	90°, 45°	90°, 80°
Interference 1 (θ,ϕ)	25°, 45°	20°, 80°
Interference 2 (θ,ϕ)	50°, 45°	130°, 80°
Interference 3 (θ,ϕ)	70°, 45°	150°, 80°
Interference 4 (θ,ϕ)	158°, 45°	160°, 80°

This article has been accepted for publication in a future issue of this journal, but has not been fully edited. Content may change prior to final publication. Citation information: DOI 10.1109/ACCESS.2018.2889877, IEEE Access

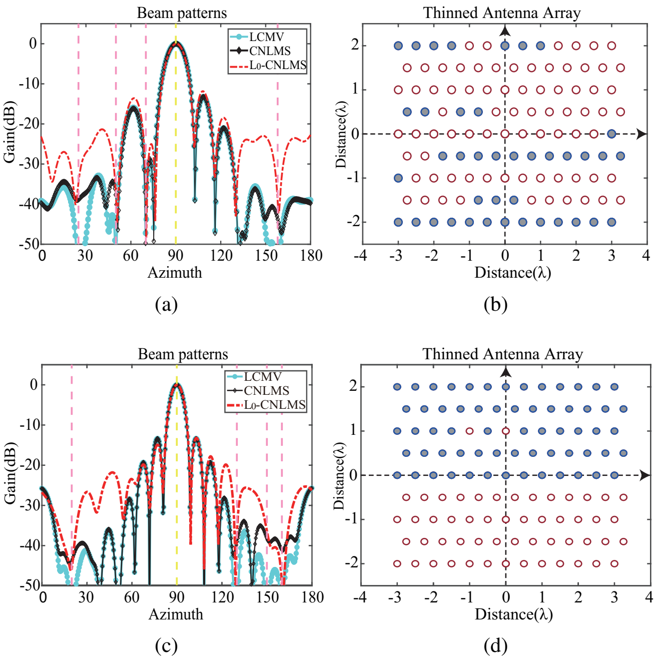

FIGURE 8: TA simulations: The beam patterns for L_0-CNLMS compared with CNLMS and LCMV algorithms. The thinned array at iteration $k = 3 \times 10^3$. (a) Simulation I: Beam patterns, (b) Simulation I: Array sparsity = 34.2%, (c) Simulation II: Beam patterns, (d) Simulation II: Array sparsity = 53.8%.

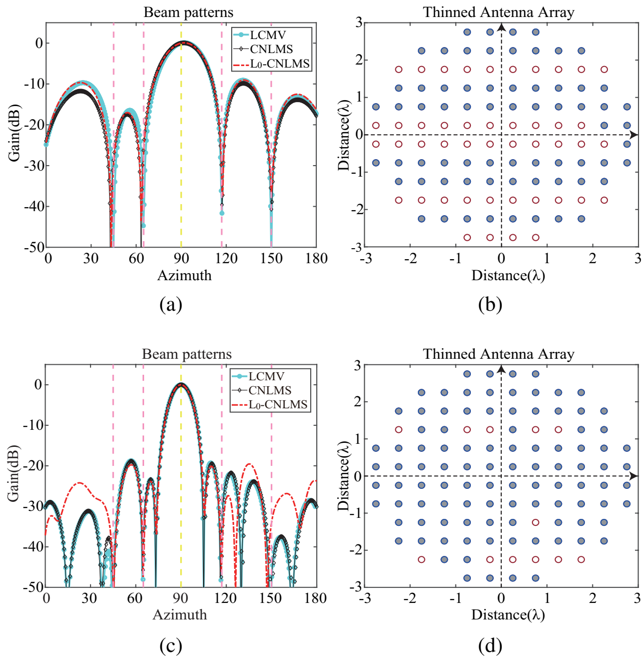

FIGURE 9: IA simulations: The beam patterns for L_0-CNLMS compared with CNLMS and LCMV algorithms. The thinned array at iteration $k = 3 \times 10^3$. (a) Simulation I: Beam patterns, (b) Simulation I: Array sparsity =59.8%, (c) Simulation II: Beam patterns, (d) Simulation II: Array sparsity =89.2%.

D. IRREGULAR ARRAY (IA)

TABLE 5: Parameter values for IA simulations

Parameter	I	II
L_0-CNLMS step-size (μ_0)	8.5×10^{-4}	8.5×10^{-4}
β	19	19
Elements' interval	$\lambda/2$	$\lambda/2$
l_0-NC	0.6	0.9
Signals' frequencies	3 GHz	3.5 GHz
SOI SNR (dB)	20	20
Interferences SNR (dB)	40	40
SOI direction (θ,ϕ)	90°, 20°	90°, 50°
Interference 1 (θ,ϕ)	45°, 20°	45°, 50°
Interference 2 (θ,ϕ)	65°, 20°	65°, 50°
Interference 3 (θ,ϕ)	117°, 20°	117°, 50°
Interference 4 (θ,ϕ)	150°, 20°	150°, 50°

In the fourth simulation, we study an IA working at S-band. Here, the IA is a 112-element rectangular array with circular boundary. Parameters of the simulations are given in Table 5.

The simulation results show similar performances as the above cases (Fig. 9) which means the proposed algorithm can deal with different applications and control the sparsity.

E. INVESTIGATION AND COMPARISON OF THE L_0-CNLMS

Herein, we present the performance of the L_0-CNLMS in comparison with the L_1-WCNLMS algorithm to verify its benefits and improvements. An X-band SHA is used to analyze the proposed method in these experiments.

TABLE 6: Comparison in small sparse ratio

Parameter	I	II
L_0-CNLMS step-size (μ_0)	8×10^{-4}	8×10^{-4}
L_1-CNLMS step-size (μ_0)	5×10^{-4}	5×10^{-4}
β for L_1-WCNLMS	20	20
β for L_0-CNLMS	20	20
Elements' interval	$\lambda/2$	$\lambda/2$
l_0-NC	0.4	0.6
l_1-NC	0.88	0.88
Signals' frequencies	8 GHz	8 GHz
SOI SNR (dB)	20	20
Interferences SNR (dB)	40	40
SOI direction (θ,ϕ)	90°, 45°	90°, 45°
Interference 1 (θ,ϕ)	22°, 45°	22°, 45°
Interference 2 (θ,ϕ)	52°, 45°	52°, 45°
Interference 3 (θ,ϕ)	80°, 45°	75°, 45°
Interference 4 (θ,ϕ)	147°, 45°	147°,45°

1) Small sparse ratio

For small sparse ratio, the parameters listed in Table 6 are used to investigate the behaviors of the L_0-CNLMS and the simulation results are given in Figs. 10 and Fig. 11. For the case I, as we can see from Fig. 10, L_1-WCNLMS finally achieves a sparse solution after 2×10^4 times of iterations, while the proposed L_0-CNLMS converges at 3×10^3 times. This means L_0-CNLMS achieves a higher level of sparsity faster than L_1-WCNLMS. It is also observed that the SLL

This article has been accepted for publication in a future issue of this journal, but has not been fully edited. Content may change prior to final publication. Citation information: DOI 10.1109/ACCESS.2018.2889877, IEEE Access

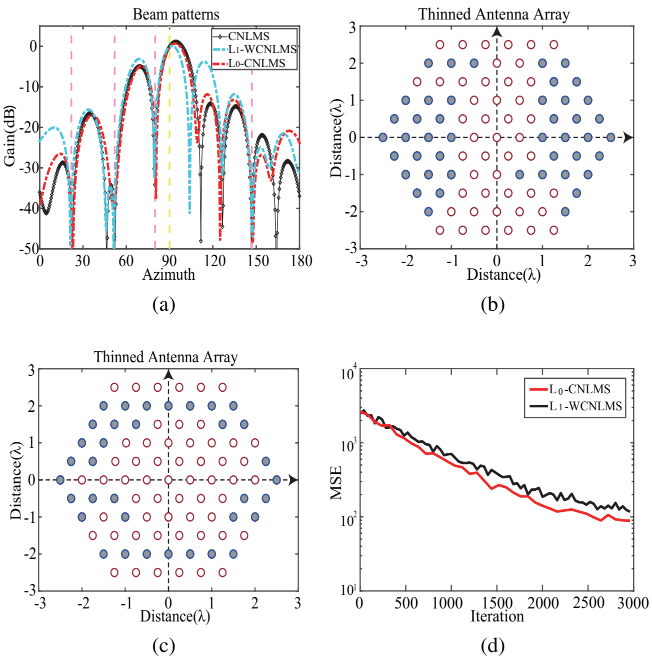

FIGURE 10: Comparison of L_0-CNLMS and L_1-WCNLMS in small sparse ratio, Case I: (a) The beam patterns for L_0-CNLMS compared with L_1-WCNLMS and CNLMS algorithms. (b) The thinned array for L_1-WCNLMS at iteration $k = 2 \times 10^4$, array sparsity = 49.5%, (c) The thinned array for L_0-CNLMS at iteration $k = 3 \times 10^3$, array sparsity = 38.5%, (d) Comparison of MSE performance of L_0-CNLMS and L_1-WCNLMS

in the L_1-WCNLMS is higher than that of the L_0-CNLMS although the L_1-WCNLMS employs much more elements. That is to say, the L_0-CNLMS can achieve better beam pattern performance with fewer antennas.

For case II, we change the directions of interferences. From Fig. 11, it is found that the L_1-WCNLMS fails to get the sparse solution and has the same beam pattern with the CNLMS. On the contrary, L_0-CNLMS can still successfully get the sparse solution. Fig. 11 (c) and (d) illustrate the reason why L_1-WCNLMS may lose the sparse solution. It can be seen that the L_1-WCNLMS algorithm has already converged and its coefficients don't change any more after 5×10^3 iterations, since the l_1-NC forces all the coefficients to small uniformly. From the comparisons, we found that the L_0-CNLMS algorithm is stable and robust when it is used for dealing with the sparse antenna array beamforming.

2) Large sparse ratio

When the sparse ratio is large, our proposed L_0-CNLMS shows more stable beam patterns then those of L_1-WCNLMS, making it more suitable for various engineering applications. For obtaining the comparison results, the simulation parameters are presented in Table 7 and the simulations are shown in Fig. 12. It turns out that the L_0-CNLMS shows

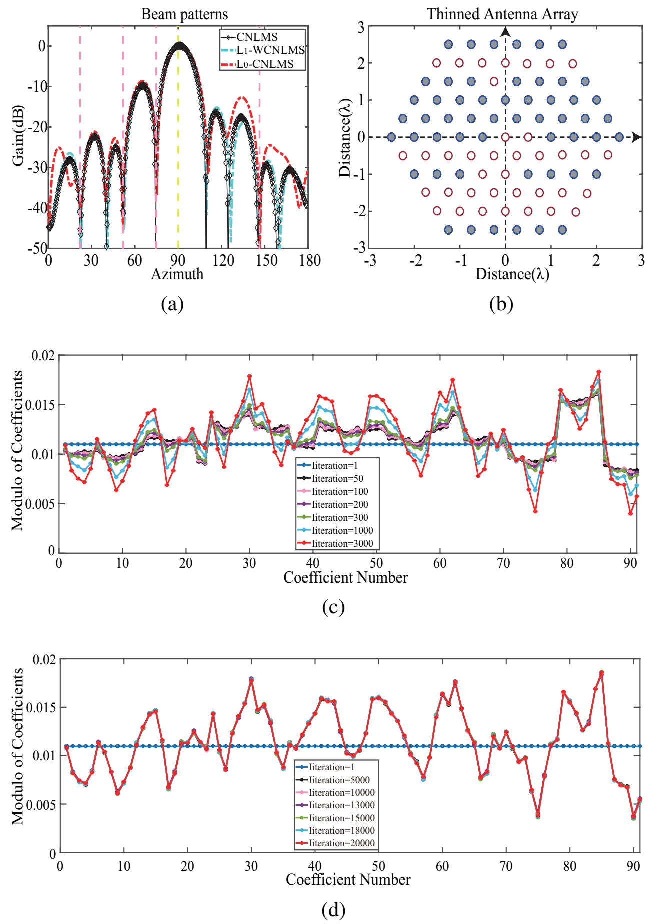

FIGURE 11: Comparison of L_0-CNLMS and L_1-WCNLMS in small sparse ratio, Case II: (a) The beam patterns for L_0-CNLMS compared with L_1-WCNLMS and CNLMS algorithms. (b) The thinned array for L_0-CNLMS at iteration $k = 3 \times 10^3$, array sparsity = 59.3%, (c) Coefficients in working process, iteration k from 1 to 3×10^3, (d) Coefficients in working process, iteration k from 5×10^3 to 2×10^4.

TABLE 7: Comparison in big sparse ratio

Parameter	I
L_0-CNLMS step-size (μ_0)	8×10^{-4}
L_1-CNLMS step-size (μ_0)	5×10^{-4}
β for L_0-CNLMS	20
β for L_1-WCNLMS	20
Elements' interval	$\lambda/2$
l_0-NC	0.2
l_1-NC	0.84
Signals' frequencies	8 GHz
SOI SNR (dB)	20
Interferences SNR (dB)	40
SOI direction (θ,ϕ)	90°, 45°
Interference 1 (θ,ϕ)	36°, 45°
Interference 2 (θ,ϕ)	65°, 45°
Interference 3 (θ,ϕ)	120°, 45°
Interference 4 (θ,ϕ)	159°, 45°

a better performance in terms of the beam patterns and MSE for the same experiment conditions.

Several experiments are carried out to verify the stabi-

This article has been accepted for publication in a future issue of this journal, but has not been fully edited. Content may change prior to final publication. Citation information: DOI 10.1109/ACCESS.2018.2889877, IEEE Access

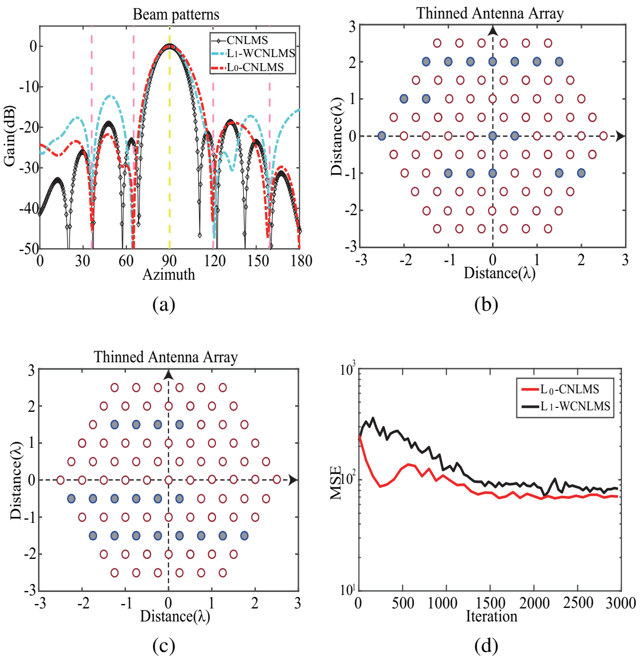

FIGURE 12: Comparison of L_0-CNLMS and L_1-WCNLMS in big sparse ratio, Simulation: (a) The beam patterns for L_0-CNLMS compared with L_1-WCNLMS and CNLMS algorithms, (b) The thinned array for L_1-WCNLMS at iteration $k = 3 \times 10^3$, array sparsity = 18.7%, (c) The thinned array for L_0-CNLMS at iteration $k = 3 \times 10^3$, array sparsity = 19.8%, (d) Comparison of MSE performance for L_0-CNLMS and L_1-WCNLMS.

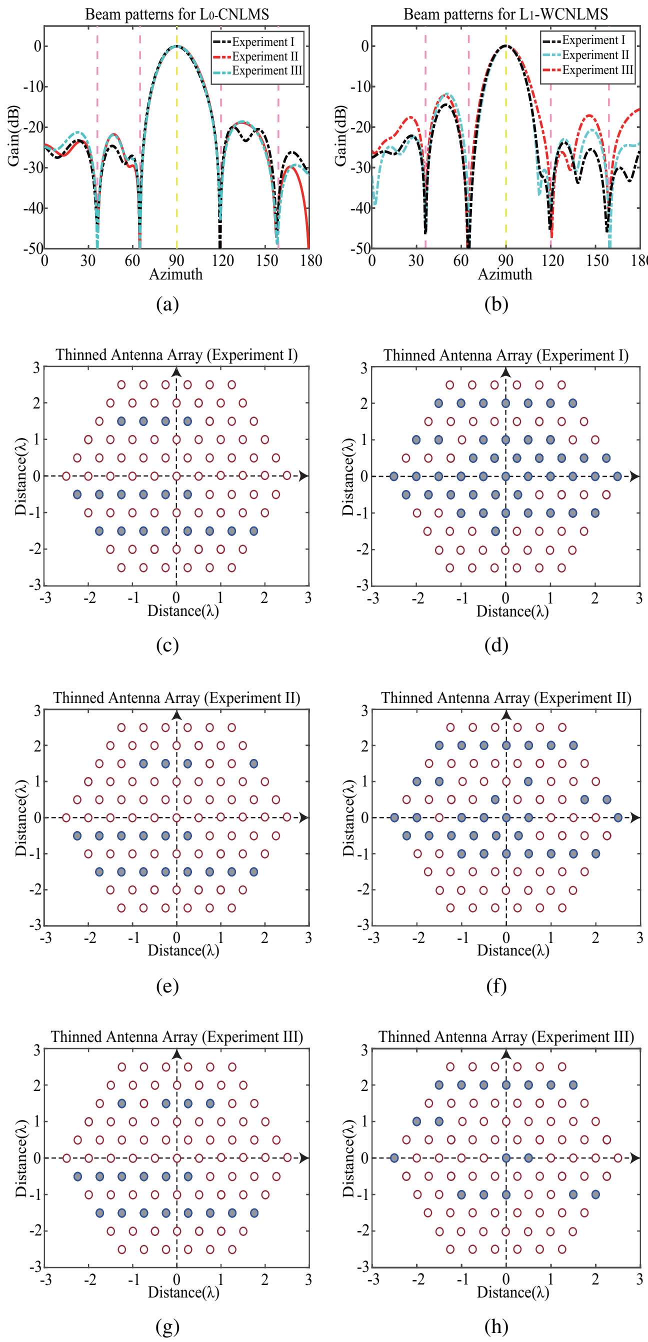

FIGURE 13: Multiple simulations of L_0-CNLMS and L_1-WCNLMS in big sparse ratio, (a), (b): Beam patterns for L_0-CNLMS and L_1-WCNLMS under multiple simulations, respectively. (c), (e) and (g): The antenna array thinned by L_0-CNLMS of which the sparsities are 19.8%, 19.8% and 19.8%, respectively. (d), (f) and (h): The antenna array thinned by L_1-WCNLMS of which the sparsities are 49.5%, 36.3% and 18.7%, respectively.

lization of L_0-CNLMS and L_1-WCNLMS algorithms. We can draw a conclusion from Fig. 13 that the beam patterns for L_0-CNLMS are much more stable than those of the L_1-WCNLMS based beam patterns. Especially, the L_0-CNLMS has the same shape for the main lobe in different experiments. Also, the sparsity of the L_1-WCNLMS varies from 18.7% to 49.5%, while the L_0-CNLMS has the stable sparsity which can get a high accuracy.

VII. ITERATION CONVERGENCE ANALYSIS

In this section, we provide the convergence analysis of the proposed L_0-CNLMS algorithm. Herein, we consider $\mathbf{w}_o$ as the optimal coefficient vector, $\mathbf{n}_k$ as the noise. Also, we define the coefficient error as $\Delta\mathbf{w}_k = \mathbf{w}_k - \mathbf{w}_o$. In this case, the priori error in the k^{th} iteration can be described as:

$$e_k = \mathbf{x}_k^{\mathrm{H}}\mathbf{w}_o + \mathbf{n}_k - \mathbf{x}_k^{\mathrm{H}}\mathbf{w}_k = \mathbf{n}_k - \mathbf{x}_k^{\mathrm{H}}\Delta\mathbf{w}_k. \tag{40}$$

Substituting μ_k into the final updating function of the proposed algorithm in equation (38), we obtain:

$$\mathbf{w}_{k+1} = \mathbf{w}_k + \frac{\mu_0}{\varepsilon_k}[e_k - \mathbf{f}_{L_0}^{\mathrm{H}}(k)\mathbf{x}_k]\mathbf{Q} + \mathbf{f}_{L_0}(k), \tag{41}$$

where $\varepsilon_k = \mathbf{Q}^{\mathrm{H}}\mathbf{x}_k$ is a scalar.

Taking $\mathbf{f}_{L_0}(k)$ into consideration, (41) can be rewritten as:

$$\mathbf{w}_{k+1} = \mathbf{w}_k + [\mathbf{I} - \frac{\mu_0}{\varepsilon_k}\mathbf{Q}\mathbf{x}_k^{\mathrm{H}}]\mathbf{f}_{L_0}(k) + \frac{\mu_0}{\varepsilon_k}e_k^*\mathbf{Q}. \tag{42}$$

Next, Substituting (40) into (42), we get

$$\begin{aligned}\mathbf{w}_{k+1} =&\mathbf{w}_k + [\mathbf{I} - \frac{\mu_0}{\varepsilon_k}\mathbf{Q}\mathbf{x}_k^{\mathrm{H}}]\mathbf{f}_{L_0}(k)\\ &+ \frac{\mu_0}{\varepsilon_k}(\mathbf{n}_k^* - \mathbf{x}_k^{\mathrm{H}}\Delta\mathbf{w}_k)\mathbf{Q}.\end{aligned} \tag{43}$$

Notice that $\mathbf{f}_{L_0}(k) = (t - \mathbf{J}_k^{\mathrm{H}}\mathbf{w}_k)(\frac{\mathbf{PJ}_k}{m})$. In the proposed algorithm, we use the constraint that $\mathbf{J}_k^{\mathrm{H}}\mathbf{w}_{k+1} = t$, i.e., the equation $\mathbf{J}_k^{\mathrm{H}}\mathbf{w}_o = t$ is satisfied when the algorithm is converged. Using his method, $\mathbf{f}_{L_0}(k)$ can also be expressed as:

$$\begin{aligned}\mathbf{f}_{L_0}(k) &= (\mathbf{J}_k^{\mathrm{H}}\mathbf{w}_o - \mathbf{J}_k^{\mathrm{H}}\mathbf{w}_k)(\frac{\mathbf{PJ}_k}{m})\\ &= -\mathbf{J}_k^{\mathrm{H}}\Delta\mathbf{w}_k(\frac{\mathbf{PJ}_k}{m})\\ &= -\mathbf{A}\Delta\mathbf{w}_k,\end{aligned} \tag{44}$$

where $\mathbf{A} = \frac{\mathbf{PJ}_k\mathbf{J}_k^{\mathrm{H}}}{m}$. Obviously, $\mathbf{A}$ is an idempotent matrix which means the eigenvalues of matrix $\mathbf{A}$ can only be 0 or 1. Also, we can easily obtain that $\mathrm{tr}[\mathbf{A}] = 1$, which is to say that matrix $\mathbf{A}$ has only one non-zero eigenvalue which equals to 1.

After substituting (44) into (43), and describing the updating equation in coefficient error form, we have:

$$\begin{aligned}\Delta\mathbf{w}_{k+1} =&\Delta\mathbf{w}_k + [\mathbf{I} - \frac{\mu_0}{\varepsilon_k}\mathbf{Q}\mathbf{x}_k^{\mathrm{H}}](-\mathbf{A}\Delta\mathbf{w}_k)\\ &+ \frac{\mu_0}{\varepsilon_k}(\mathbf{n}_k^* - \mathbf{x}_k^{\mathrm{H}}\Delta\mathbf{w}_k)\mathbf{Q}\\ =&[\mathbf{I} - \mu_0\mathbf{B}]\Delta\mathbf{w}_k - [\mathbf{I} - \mu_0\mathbf{B}]\mathbf{A}\Delta\mathbf{w}_k\\ &+ \frac{\mu_0}{\varepsilon_k}n_k^*\mathbf{Q}\\ =&[\mathbf{I} - \mu_0\mathbf{B}][\mathbf{I} - \mathbf{A}]\Delta\mathbf{w}_k + \frac{\mu_0}{\varepsilon_k}n_k^*\mathbf{Q},\end{aligned} \tag{45}$$

where $\mathbf{B} = \frac{\mathbf{Q}\mathbf{x}_k^{\mathrm{H}}}{\varepsilon_k}$. Similar to $\mathbf{A}$, $\mathbf{B}$ is also an idempotent matrix whose maximum eigenvalue is $\lambda_{\max} = 1$.

Then, we take expectations on both sides of (45), and then, we have

$$\begin{aligned}E[\Delta\mathbf{w}_{k+1}] =&E\{[\mathbf{I} - \mu_0\mathbf{B}][\mathbf{I} - \mathbf{A}]\Delta\mathbf{w}_k\}\\ &+ E[\frac{\mu_0}{\varepsilon_k}n_k^*\mathbf{Q}].\end{aligned} \tag{46}$$

Considering the independence assumption, that is, $\Delta\mathbf{w}_k$ is statistic independence with $\mathbf{n}_k$, $\mathbf{x}_k$ and $\mathbf{J}_k$ [42], and taking into account that the expectation of $\mathbf{n}_k$ is 0, we can obtain:

$$\begin{aligned}&E[\Delta\mathbf{w}_{k+1}] = [\mathbf{I} - \mu_0\mathbf{B}][\mathbf{I} - \mathbf{A}]E[\Delta\mathbf{w}_k] =\\ &[\mathbf{I} - \mu_0\mathbf{B}][\mathbf{I} - \mathbf{A} - \mu_0\mathbf{B} - \mu_0\mathbf{AB}]^k[\mathbf{I} - \mathbf{A}]E[\Delta\mathbf{w}_0]\end{aligned} \tag{47}$$

Note that $\mathbf{AB} = \mathbf{0}$, and thus (47) can be rewritten as:

$$E[\Delta\mathbf{w}_{k+1}] = [\mathbf{I}-\mu_0\mathbf{B}][\mathbf{I}-\mathbf{A}-\mu_0\mathbf{B}]^k[\mathbf{I}-\mathbf{A}]E[\Delta\mathbf{w}_0] \tag{48}$$

In the discussions above, we have concluded that matrices $\mathbf{A}$ and $\mathbf{B}$ have the same eigenvalues, of which $N-1$ are equal to 0 and the other one is 1. Thus, if μ_0 satisfies $|1-1-\mu_0| < 1$ and $|1-0-\mu_0| < 1$, the algorithm will converge. In this case, we have

$$0 < \mu_0 < 1, \tag{49}$$

while the convergence domain for L_1-WCNLMS is given in [34], which is

$$0 < \mu_1 < 2. \tag{50}$$

It turns out that L_1-WCNLMS has a more widely convergence domain, but it should be pointed out that the selection of step-size for both L_0-CNLMS and L_1-WCNLMS are always far below the upper bound for a better performance [34].

VIII. CONCLUSION

In this paper, an L_0-CNLMS algorithm is proposed for adaptive beamforming as an improved version of L_1-WCNLMS in sparse antenna arrays with controllable sparsity. The results of the simulations presented in Section VI show that the proposed algorithm is suitable for sparse array beamforming in various array configurations.

The proposed algorithm can form excellent beams under different conditions, e.g., different number of signals and varying directions. Besides, the sparsity of the antenna array can be controlled by a parameter t. As such, a trade-off between the beam quality and hardware/power consumption can be achieved for any particular application and system requirement. In addition, the L_0-CNLMS algorithm converges faster and uses fewer antennas to achieve a better performance when compared with the L_1-WCNLMS algorithm. We can see from the simulation results that the proposed L_0-CNLMS algorithm is superior to the mentioned algorithms for handling sparse beamforming. The SLL of the proposed L_0-CNLMS algorithm is slightly higher than that of conventional non-sparse algorithms. For the non-sparse array, the proposed algorithm has high computations which may limit its applications. Thus, the adaptive beamforming algorithm with low complexity, low SLL and high performance should be developed in the future work to meet all the array beamforming applications.

REFERENCES

[1] O. L. Frost III, “An algorithm for linearly constrained adaptive array processing,” Proc. IEEE, vol. 60, no. 8, pp. 926-935, Aug., 1972.

[2] J. A. Apolinário, Jr., S. Werner, P. S. R. Diniz, and T. I. Laakso, “Constrained normalized adaptive filtering for CDMA mobile communications,” IEEE Signal Processing Conference, Rhodes, Greece, Sep. 1998, pp. 1-4.

[3] Y. Chen, Y. Gu, and A. O. Hero, “Sparse LMS for system identification," Proc. IEEE International Conference on Acoustic Speech and Signal Processing, (ICASSP’09), pp.3125-3128, Taipei, Taiwan, April 2009.

[4] Y. Gu, J. Jin, S. Mei, “l_0-norm constraint LMS algorithm for sparse system identification,” IEEE Signal Process. Lett., vol. 16, no. 9, pp. 774-777, Sept., 2009, 10.1109/LSP.2009.2024736.

[5] Y. Li, Y. Wang, R. Yang, et al. “A Soft Parameter Function Penalized Normalized Maximum Correntropy Criterion Algorithm for Sparse System Identification,” Entropy, vol. 19, no. 1, p. 45, Jan., 2017, 10.3390/e19010045.

[6] Y. Li, Y. Wang, T. Jiang, “Norm-adaption penalized least mean square/fourth algorithm for sparse channel estimation,” Signal Processing, vol.128, pp.243-251, Nov., 2016, 10.1016/j.sigpro.2016.04.003.

[7] O. Taheri and S. A. Vorobyov, “Sparse channel estimation with L_p-norm and reweighted L_1-norm penalized least mean squares," IEEE International Conference on Acoustic Speech and Signal Processing (ICASSP’11), pp.2864-2867, Prague, Czech Republic, May 2011.

[8] G. Gui, S. Kumagai, A. Mehbodniya, F. Adachi, "Two are better than one:adaptive sparse system idenfication using affine aombination of two sparse adaptive filters," In Proceedings of the IEEE 79th Vehicular Technology Conference (VTC2014-Spring), Seoul, Korea, 18-21 May 2014.
[9] Y. Li, C. Zhang, S. Wang, "Low complexity non-uniform penalized affine projection algorithm for sparse system identification," Circuits Syst. Signal Process, vol. 35, no. 5, pp. 1611-1624, May, 2016, 10.1007/s00034-015-0132-3.
[10] Y. Li, Y. Wang, T. Jiang, "Sparse-aware set-membership NLMS algorithms and their application for sparse channel estimation and echo cancelation," AEU-International Journal of Electronics and Communications, vol. 70, no. 7, pp. 895-902, July, 2016, 10.1016/j.aeue.2016.04.001.
[11] Y. Li, Y. Wang. F. Albu, "Sparse channel estimation based on a reweighted least-mean mixed-norm adaptive filter algorithm," Signal Processing Conference IEEE, Budapest, Hungary, Aug., 2016.
[12] Z. Yang, L. Xie, "Enhancing sparsity and resolution via reweighted atomic norm minimization," IEEE Transactions on Signal Processing, vol. 64, no. 4, pp. 995-1006, Feb. 15, Feb., 2016.
[13] Z. Yang, L. Xie, "Exact joint sparse frequency recovery via optimization methods," IEEE Transactions on Signal Processing, vol. 64, no. 19, pp. 5145-5157, Oct., 2016.
[14] R. Tibshirani, "Regression shrinkage and selection via the lasso," J. R. Stat. Soc. Ser. B-Stat. Methodol., vol.58, no.1, pp.267-288, Jan. 1996.
[15] D. L. Donoho, "Compressed sensing," IEEE Trans. Inf. Theory, vol.52, no.4, pp.1289-1306, April 2006.
[16] Z. Jin, Y. Li, J. Liu, "An Improved Set-Membership Proportionate Adaptive Algorithm for a Block-Sparse System," Symmetry, vol. 10, no. 3, p. 75, Mar., 2018, 10.3390/sym10030075.
[17] S. Jiang, Y. Gu, "Block-Sparsity-Induced Adaptive Filter for Multi-Clustering System Identification," IEEE Trans. Signal Process, vol. 63, no. 20, pp. 5318-5330, Oct., 2015, 10.1109/TSP.2015.2453133.
[18] H. Deng, M. Doroslova, "Improving convergence of the PNLMS algorithm for sparse impulse response identification," IEEE Signal Process. Lett., vol. 12, no. 3, pp. 181-184, Feb., 2005, 10.1109/LSP.2004.842262.
[19] B. Babadi, N. Kalouptsidis, V. Tarokh, "SPARLS: The sparse RLS algorithm", IEEE Transactions on Signal Processing, vol. 58, no. 8, pp. 4013-4025, Aug., 2010, 10.1109/TSP.2010.2048103.
[20] P. D. Lorenzo, A. H. Sayed, "Sparse Distributed Learning Based on Diffusion Adaptation," IEEE Transactions on Signal Processing, vol. 61, no. 6, pp. 1419-1433, Dec., 1996, 10.1109/TSP.2012.2232663.
[21] D. Angelosante, J. A. Bazerque, G. B. Giannakis, "Online Adaptive Estimation of Sparse Signals: Where RLS Meets the l_1-Norm," IEEE Transactions on Signal Processing, vol. 58, no. 7, pp. 3436-3447, Mar., 2010, 10.1109/TSP.2010.2046897.
[22] G. Gui, W. Peng, F. Adachi, "Improved adaptive sparse channel estimation based on the least mean square algorithm," Wireless Communications and Networking Conference (WCNC),2013 IEEE, Shanghai, China, 2013, pp. 3105-3109.
[23] K. Shi, P. Shi, "Convergence analysis of sparse LMS algorithms with l_1-norm penalty based on white input signal," Signal Processing, vol. 90, no. 12, pp. 3289-3293, Dec., 2010, 10.1016/j.sigpro.2010.05.015.
[24] Y. Wang, Y. Li, Z. Jin, "An improved reweighted zero-attracting NLMS algorithm for broadband sparse channel estimation," IEEE International Conference on Electronic Information and Communication Technology, Harbin, China, Aug., 2016.
[25] D. L. Duttweiler, "Proportionate normalized least-mean-squares adaptation in echo cancelers," IEEE Trans. Speech Audio Process, vol. 8, no. 5, pp. 508-518, Sept., 2000, 10.1109/89.861368.
[26] Y. Li, Z. Jin, Y. Wang, "Adaptive channel estimation based on an improved norm constrained set-membership normalized least mean square algorithm," Wirel. Commun. Mobile Comput. 2017(1):1-8, Jan., 2017, 10.1155/2017/8056126.
[27] G. Gui, A. Mehbodniya, F. Adachi, "Least mean square/fourth algorithm for adaptive sparse channel estimation," In Proceedings of the 24th IEEE International Symposium on Personal Indoor and Mobile Radio Communications (PIMRC), London, UK, 2013, pp. 296-300.
[28] Y. Li, Y. Wang, T. Jiang, "Sparse channel estimation based on a p-norm-like constrained least mean fourth algorithm," In Proceedings of the 7th International Conference on Wireless Communications and Signal Processing (WCSP), Nanjing, China, 2015, pp.1-4.
[29] Y. Li, M. Hamamura, "Zero-attracting variable-step-size least mean square algorithms for adaptive sparse channel estimation," Int. J. Adapt. Control Signal Process, vol. 29, no. 9, pp. 1189-1206, Sept., 2015, 10.1002/acs.2536.
[30] Y. Li, M. Hamamura, "An improved proportionate normalized least-mean-square algorithm for broadband multipath channel estimation," Sci. World J, Mar., 2014, 10.1155/2014/572969.
[31] Y. Wang, Y. Li, R. Yang, "Sparse adaptive channel estimation based on mixed controlled l 2 and lp -norm error criterion," J. Frankl. Inst., vol. 345, no. 15, pp. 7215-7239, Oct., 2017, 10.1016/j.jfranklin.2017.07.036.
[32] S. L. Gay, "An efficient, fast converging adaptive filter for network echo cancellation," In Proceedings of the Conference Record of the Thirty-Second Asilomar Conference on Signals, Systems Computers, Pacific Grove, CA, USA, 1998, pp. 394-398.
[33] J. Liu, S.L. Grant, "Block sparse memory improved proportionate affine projection sign algorithm," Electron. Lett, vol. 51, no. 24, pp. 2001-2003, Nov., 2015, 10.1049/el.2015.3066.
[34] J. F. de Andrade, M. L. R. de Campos, J. A. Apolinário, "L_1-Constrained Normalized LMS Algorithms for Adaptive Beamforming," IEEE Transactions on Signal Processing, vol.63, no.24, pp.6524-6539, Dec., 2015, 10.1109/TSP.2015.2474302.
[35] J. Liu, W. Zhou, F. H. Juwono, D. Huang, "Reweighted smoothed l_0-norm based DOA estimation for MIMO radar," Signal Processing, vol.137, pp.44-51, Aug., 2017, 10.1016/j.sigpro.2017.01.034.
[36] C. S. Oxvig, P. S. Pedersen, T. Arildsen, et al. "Improving Smoothed l_0 Norm in Compressive Sensing Using Adaptive Parameter Selection." Mathematics, 2013.
[37] M. V. S. Lima, T. N. Ferreira, W. A. Martins, P. S. R. Diniz, "Sparsity-Aware Data-Selective Adaptive Filters," IEEE Transactions on Signal Processing, vol. 62, no. 17, pp. 4557-4572, July, 2014, 10.1109/TSP.2014.2334560.
[38] B. Chen, L. Xing, J. Liang, N. Zheng and J. C. Principe, "Steady-state Mean-square Error Analysis for Adaptive Filtering under the Maximum Correntropy Criterion," IEEE Signal Processing Letters, vol. 21, no. 7, pp. 880-884, 2014, 10.1109/LSP.2014.2319308.
[39] A. V. Shishlov, "Vehicular antennas for satellite communications," in Proc. VIII Int. Conf. Antenna Theory Tech. (ICATT), Kyev, Ukraine,Sep. 2011, pp. 34-39.
[40] R. S. Wexler, R. Hoffmann, R. Collins, and P. Moran, "Successful development and test of SATCOM on-the-move (OTM) Ku-band Ka-band systems for the armyąŕs warfighter information network-tactical (WIN-T)," in Proc. IEEE Military Commun. Conf. (MILCOM), Washington, DC, USA, Oct. 2006, pp. 1-7.
[41] P. S. Bradley, O. L. Mangasarian, "Feature Selection via Concave Minimization and Support Vector Machines," Proc. 13th ICML, San Francisco, CA, USA, 1998, pp. 82-90.
[42] P. S. R. Diniz, Adaptive Filtering: Algorithms and Practical Implementation, New York, USA: Springer, 2010.
[43] J. F. de Andrade, M. L. R. de Campos, J. A. Apolinário "An L_1-norm linearly constrained LMS algorithm applied to adaptive beamforming," in Proc. 7th IEEE Sensor Array Multichannel Signal Process. Workshop (SAM), Hoboken, NJ, USA, 2012, pp. 429-432.

WANLU SHI was born in Daqing, Heilongjiang Province, P. R. China in 1992. He received the B.S. degree in information and communication engineering from Harbin Engineering University in 2015. He is pursuing his Ph. D. degree and his projects are sparse signal processing and adaptive beamforming.

From 2015 to 2016, he was an Assistant Engineer of the 14th Institute of China Electronics Technology Group.

YINGSONG LI received his B.S. degree in electrical and information engineering in 2006, and M.S. degree in Electromagnetic Field and Microwave Technology from Harbin Engineering University, 2006 and 2011, respectively. He received his Ph.D degree from both Kochi University of Technology (KUT), Japan and Harbin Engineering University, China in 2014.

He is a visiting scholar of University of California, Davis from March 2016 to March 2017. Now, he is a full professor of Harbin Engineering University from July 2014. He is also a visiting professor of Far Eastern Federal University (FEFU) and KUT. He is a senior of Chinese Institute of Electronics (CIE), member of IEEE. He is an Associate Editor of IEEE Access and AEÜ- International Journal of Electronics and Communications.

Dr. Li also serves as a reviewer for more than 20 journals. Recently, his recent research interests are mainly in remote sensing, underwater communications, signal processing, radar, SAR imaging, compressed sensing and antennas.

LUYU ZHAO was born in Xi'an, China, in 1984. He received the B.Eng. degree from Xidian University, Xi'an, China in 2007, and the Ph. D. degree from The Chinese University of Hong Kong, Shatin, Hong Kong in 2014. He has been an associate professor at the National Key Laboratory of Antennas and Microwave Technology, Xidian University since 2016.

From 2007 to 2009, he was with the Key Laboratory of Antennas and Microwave Technology, Xidian University, as a Research Assistant, where he was involved with software and hardware implementation of RF identification (RFID) technologies. From 2014 to 2015, he was a Postdoctoral Fellow at The Chinese University of Hong Kong, Shatin, Hong Kong. From Oct. 2015 to Oct. 2016, he was with Wyzdom Wireless Co. Ltd., where he was a co-founder and CTO.

His current research interests include design and application of multiple antenna systems for next generation mobile communication systems, innovative passive RF and microwave components and systems, millimeter wave and terahertz antenna array, meta-material based or inspired antenna arrays.

Dr. Zhao was the recipient of the Best Student Paper Award of 2013 IEEE 14th HK AP/MTT Postgraduate Conference. The Honorable Mention Award of 2017 Asia-Pacific Conference on Antenna and Propagation.

XIAOGUANG "LEO" LIU received the bachelor's degree from Zhejiang University, Hangzhou, China, in 2004, and the Ph.D. degree from Purdue University, West Lafayette, IN, USA, in 2010.

He joined the Department of Electrical and Computer Engineering, University of California at Davis, Davis, CA, USA, in 2011, as an Assistant Professor and was promoted to an Associate Professor in 2017. At the University of California at Davis, his research group is investigating various aspects of cutting-edge high-frequency circuit and system design and implementation concepts. His group's website is https://dart.ece.ucdavis.edu/.